Journal of Cardiovascular Translational Research (2023) 16:1392–1407
https://doi.org/10.1007/s12265-023-10408-3

ORIGINAL ARTICLE

Comparison and Evaluation of Two Combination Modes of Angiotensin for Establishing Murine Aortic Dissection Models

Wenhui He[1] · Sanjiu Yu[2] · Haoyang Li[3] · Ping He[2] · Tiantian Xiong[1] · Chaojun Yan[2] · Jingyu Zhang[4] · Shan Chen[1] · Mei Guo[2] · Xu Tan[1] · Dan Zhong[1] · Jianbin Sun[1] · Zhizhen Xu[1] · Wei Cheng[2] · Jun Li[2]

Received: 29 December 2022 / Accepted: 22 June 2023 / Published online: 25 September 2023

Abstract

Aortic dissection (AD) is a potentially fatal cardiovascular emergency caused by separation of different layers of aortic wall. However, because of limited time window available for clinical research, there is an urgent need for an ideal animal research model. In recent years, the incidence of AD complicated by atherosclerosis has increased with improvements of living standards and changes of eating habits. Accordingly, considering multiple risk factors, we successfully and efficiently established a novel AD model through a high-fat diet combined with chronic angiotensin II (AngII) infusion. Compared with traditional chemical induction model using AngII and β-aminopropionitrile, our model is more clinically relevant for atherosclerosis-related AD. Moreover, infiltration of neutrophils and apoptosis of vascular smooth muscle cells in AD tissues were more significant. In addition to enriching the existing models, the novel model may be a long-term useful tool for more in-depth investigation of AD mechanisms and preclinical therapeutic developments.

Keywords Aortic dissection (AD) · Animal models · Atherosclerosis · Angiotensin II (AngII) · Neutrophils

Introduction

Aortic dissection (AD) is an emergent medical condition characterized by a separation of the aortic wall layers and subsequent creation of a false lumen [1]. However in terms of clinical manifestations, AD patients may not have obvious preceding symptoms. The aortic vessel walls of patients have already suffered from severe tears by the time when they are rushed to the hospital; thus, AD exhibit a high mortality if undetected [2]. Therefore, important unmet needs in AD management are unraveling of its pathogenesis, prompt diagnosis, and accurate and sensitive identification of patients at risk.

In addition to hereditary vascular disease in some patients, hypertension is the most important risk factor for AD. Compliance of aortic vascular wall decreases with age and other reasons, and the pressure of blood flow on vascular wall increases to further damage the vascular wall, resulting in a break in the aorta and eventually forming AD. With improvements in living standards and changes in eating habits, the number of patients with AD related with dyslipidemia or atherosclerosis has increased sharply. A 20-year experience of collaborative clinical research revealed that a history of atherosclerosis was present in 26.5% of patients

Associate Editor Judith C. Sluimer oversaw the review of this article

Wenhui He, Sanjiu Yu, and Haoyang Li have contributed equally to this work and share first authorship.

✉ Zhizhen Xu
gfxzz@tmmu.edu.cn

✉ Wei Cheng
yjchw21@126.com

✉ Jun Li
lj@tmmu.edu.cn

[1] Department of Biochemistry and Molecular Biology, Third Military Medical University (Army Medical University), Chongqing 400038, China

[2] Department of Cardiac Surgery, The First Affiliated Hospital of Third Military Medical University (Army Medical University), Chongqing 400038, China

[3] Brigade 5 of Medical Undergraduate, Third Military Medical University (Army Medical University), Chongqing, China

[4] Army Medical Center of PLA, Third Military Medical University (Army Medical University), Chongqing, China

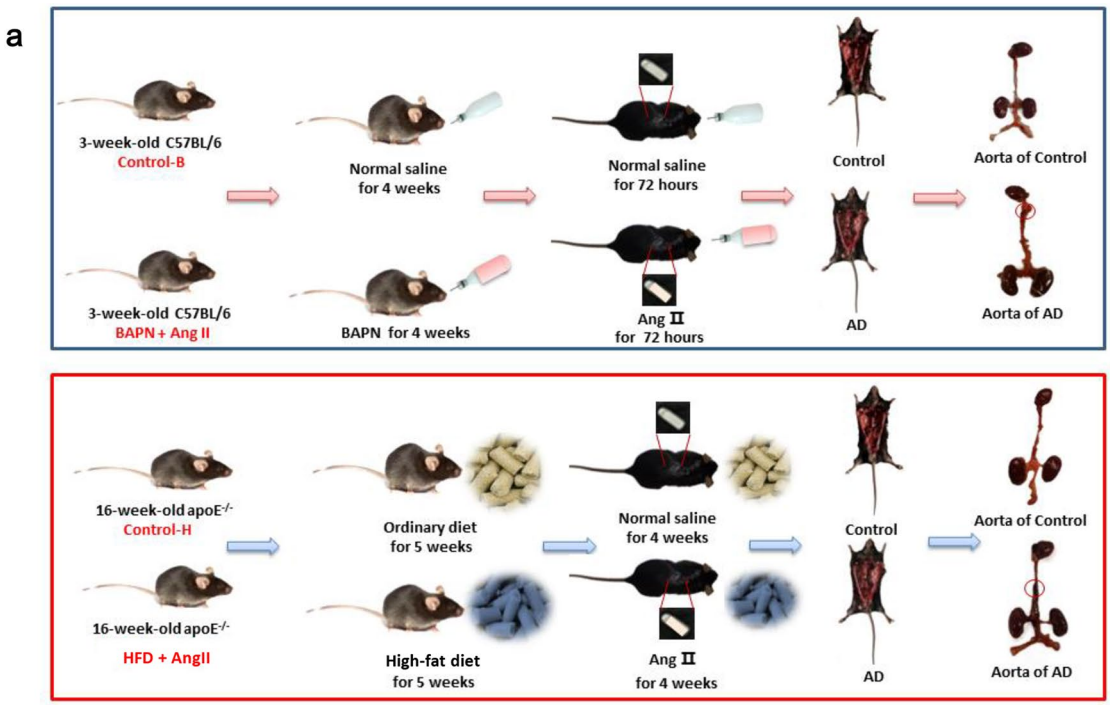
a
3-week-old C57BL/6
Control-B
Normal saline
for 4 weeks
Normal saline
for 72 hours
Control
Aorta of Control
3-week-old C57BL/6
BAPN + Ang II
BAPN for 4 weeks
Ang II
for 72 hours
AD
Aorta of AD
16-week-old apoE-/-
Control-H
Ordinary diet
for 5 weeks
Normal saline
for 4 weeks
Control
Aorta of Control
16-week-old apoE-/-
HFD + AngII
High-fat diet
for 5 weeks
Ang II
for 4 weeks
AD
Aorta of AD

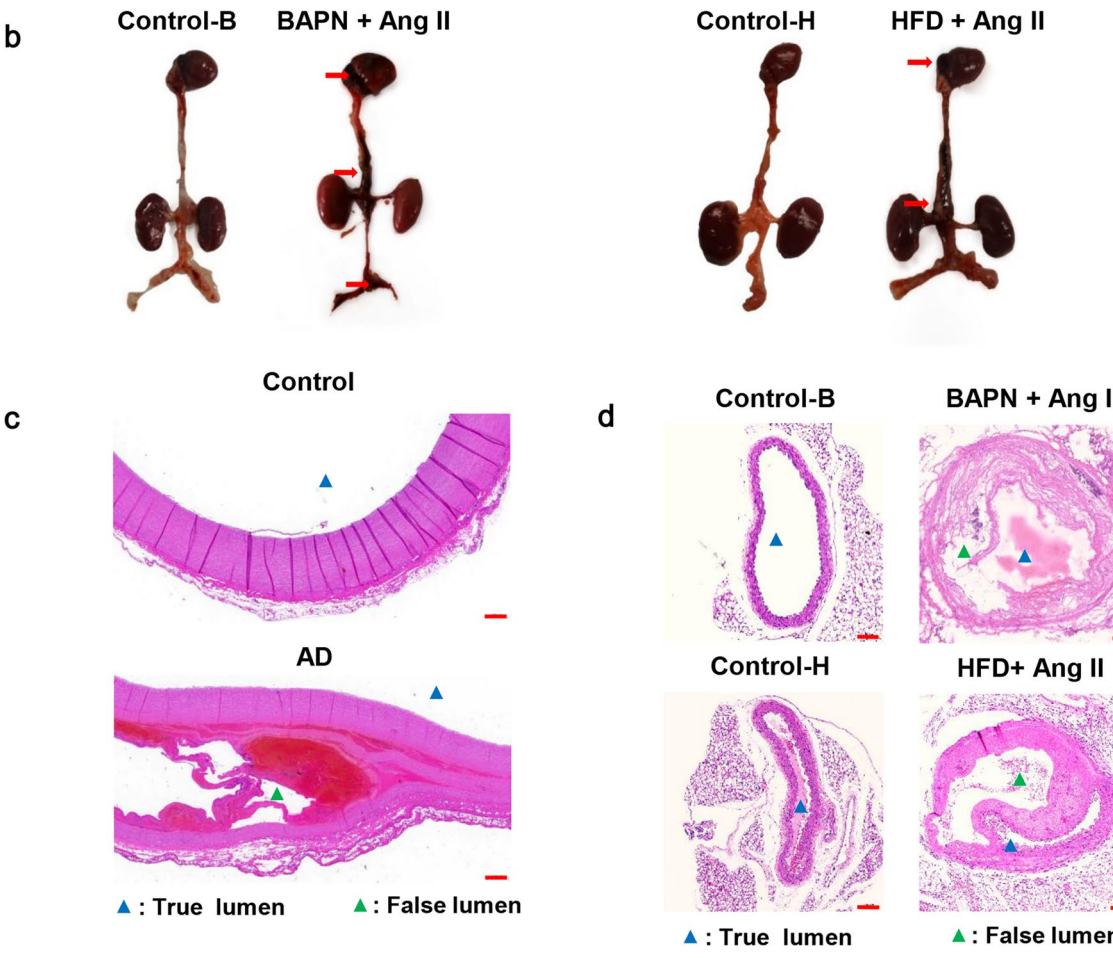
b
Control-B
BAPN + Ang II
Control-H
HFD + Ang II
c
Control
AD
▲: True lumen
▲: False lumen
d
Control-B
BAPN + Ang II
Control-H
HFD+ Ang II
▲: True lumen
▲: False lumen

◂**Fig. 1** Establishment and evaluation of the two kinds of AD models in mice. **a** Construction strategies for the two kinds of murine AD model. The details of animal grouping and model preparation are described in "Materials and Methods" in the manuscript. **b** Gross observation of aorta. The heart, aortic vessels, and kidneys of each group of mice were separated, and the two intervention groups had swollen blood clots in different parts. **c** Hematoxylin–eosin (HE) staining to show dissection (AD) and non-dissection (Control) part of blood vessels of AD patient. Numerous red blood cells infiltrated the false lumen (green arrow) of the dissection site. Scale bars, 500 μm. **d** HE staining of aorta tissues from murine models. Two kinds of intervention resulted in dissection and blood within the aortic media, while no false lumen was found in the blood vessels of corresponding control mice and the vascular structure was intact. Scale bars, 100 μm. Control-B: control group of "BAPN + AngII" group; Control-H: control group of "HFD + AngII" group; $n = 15$

among the 7300 cases provided by the International Registry of Acute Aortic Dissection (IRAD), becoming the second major risk [3]. Accordingly, this kind of AD can be considered an "atherosclerotic" acute aortic syndrome [4]. Moreover, increasing clinical and research data have shown a bidirectional association between atherosclerosis and hypertension [5, 6], which have the potential to synergistically promote AD progression. Better understanding of the cross-interaction will allow broadening the therapeutic options available for patients or preventive strategies.

Besides the complex etiology, there are still many difficulties in studies on AD, such as limited time window available for clinical research. AD patients are usually critically ill, their condition progresses very rapidly, and they often require emergency surgical treatment; otherwise, there is a 50% chance of death within the first 48 h [7]. Therefore, it is difficult to study disease progression and perioperative drug intervention. Moreover, it is hard to obtain specimens. Only patients undergoing open surgery can be the source of aortic samples. Specimens cannot be obtained non-invasively or minimally; therefore, large-scale controlled clinical trials are difficult to perform. Undoubtedly, an ideal animal model that mimics the human anatomy and pathophysiology is a powerful tool for studying AD mechanisms and preclinical therapeutic developments.

Several experimental animal models of AD have been generated, such as surgically caused, genetically modified, and pharmacologically induced models [8]. Currently, most murine models are based on chemical induction of angiotensin II (AngII) and β-aminopropionitrile (BAPN), which may be the optimum models mimicking the pathological process of AD caused by hypertension [9]. However, no single experimental model has been sufficient in investigating the pathogenesis and treatment of AD. As mentioned above, the incidence of AD related to dyslipidemia and atherosclerosis is increasing. Therefore, there is an urgent need to develop a stable and efficient AD murine model with consideration of multiple risk factors.

In this study, we established a novel AD murine model by using high-fat diet (HFD) combined with chronic AngII intervention, taking into account such things as age, vascular atherosclerosis, and hypertension. Additionally, we compared and analyzed this model with the traditional chemical induction model with AngII and BAPN. Our aim is to provide a stable and useful tool for analyzing the underlying mechanism of progression, which could thus be beneficial for therapeutics.

Materials and Methods

Patient Specimens and Ethics Statement

Dissection samples and control aorta from the non-dissection part of the same patient were collected from an AD patient with a history of atherosclerosis, who had undergone repair surgery at the First Affiliated Hospital of the Army Medical University (the additional information about the patient is listed in Supplementary Table 1). Informed consent was obtained for the use of the specimens. The use of human tissue was approved by the Ethical Committee of the First Affiliated Hospital of the Army Medical University (No.KY2019159) and the study complied with the principles outlined in the Declaration of Helsinki.

Animal Model and Ethics Statement

The strategy for the construction of the two AD models is outlined in Fig. 1a. The study was reviewed and approved by the Laboratory Animal Welfare and Ethics Committee of Army Medical University (AMUWEC20211847).

Thirty 3-week-old male C57BL/6 mice (purchased from Beijing Huafukang Biotechnology Co., Ltd.) were randomly divided into the "BAPN + AngII" intervention group and corresponding control group ("Control-B") using a random number allocation method, with 15 mice in each group. For convenience of observation, each group of mice was kept in three cages, five in each litter. We then weighed and recorded the weight of the mice in units of litter. BAPN was dissolved in the drinking water of the mice in the "BAPN + AngII" group at a dose of 1 g/kg/day, and the mice in the "Control-B" group were given ordinary drinking water. After 4 weeks of BAPN intervention, the mice in the "BAPN + AngII" group were implanted with micropumps (Alzetmodel1003D, Durect Corp., USA) that delivered AngII subcutaneously at a dose of 1000 ng/kg/min, while those in the "Control-B" group were implanted with micropumps with saline, as described previously [10]. The mice were euthanized after 72 h (BAPN was continued in the drinking water during AngII infusion).

Similarly, 30 male, 16-week-old, apolipoprotein E-deficient (apoE-/-) mice (backcrossed 10 times onto a C57BL/6 background, obtained from Beijing Huafukang Biotechnology Co., Ltd.) were randomly divided into the "HFD + AngII" intervention group and corresponding control group ("Control-H"). The "HFD + AngII" group mice were fed with HFD (D12109C, Ready Bite, China, 0.5 g/per mouse/every day, 40% fat, 1.25% cholesterol, 0.5% sodium cholate), while those in the "Control-H" group were fed with ordinary diet. After high-fat feeding for 5 weeks, the mice in the "HFD + AngII" group were implanted with micropumps (Alzet 2004, Durect Corp., USA) that delivered AngII subcutaneously at a dose of 1000 ng/kg/min, while those in the "Control-H" group were implanted with micropumps with saline, as described above. The mice were euthanized after 4 weeks (HFD was continued during AngII infusion).

Evaluation of Artic Dissection and Classification

The animals were sacrificed after anesthesia; the heart-aorta-kidney tissues were stripped to calculate the incidence of dissection. Aortic dissection was defined as the presence of hematoma within the aortic wall detected on gross examination, or as the presence of layer separation within the aortic media or medial-adventitial boundary (with a false lumen hematoma) detected on aortic histology [11]. Aortic rupture and premature death were documented. AD can be classified according to the segments involved; the Debakey system and the Stanford system are the two most commonly used classifications [12, 13]. Vascular tissues were evaluated by 3 independent observers (in the case of a discrepancy, the observers discussed and came to an agreement). More typical pathological alterations of the aorta were characterized by various histology staining.

Pathological Specimen Preparation and Staining

Human specimens and murine aorta samples were divided into two groups. One group of fresh tissues was directly embedded with medium optimal cutting temperature compound to quickly frozen, and sliced with a microtome for 7 μm. The frozen sections were stored at − 80 °C for later use. The other group of tissues was fixed in 4% paraformaldehyde and for conventional paraffin embedding, also cut into slices for later use. Then, the paraffin sections were used for hematoxylin–eosin (HE) staining, Masson staining, Victoria blue (VB) staining, and TUNEL staining, whereas the frozen sections were used for Oil Red O staining and immunofluorescence tests.

Hematoxylin-Eosin (HE) Staining

The prepared paraffin sections were baked, dewaxed, hydrated, and incubated in hematoxylin solution for 10 min. Then, they were differentiated in alcoholic hydrochloric acid for 15 s and blued in Scott bluing buffer for 15 s. They were washed and incubated in eosin solution for 2 min, dehydrated and permeabilized with xylene afterwards. Eventually, the slides were mounted with a neutral resin, observed under a microscope, and photographed.

Masson Staining

The paraffin sections were deparaffinized, and the cell nuclei were stained with hematoxylin staining solution for 10 min. Then, they were differentiated in alcoholic hydrochloric acid for 10 s and blued in Masson buffer for 10 min. After immersed in glacial acetic acid aqueous for 5 s, they were differentiated with a 1% phosphomolybdic acid aqueous solution for 3–5 min, dyed with aniline blue for 5 min. Finally, they were dehydrated, transparentized, mounted, and observed under a microscope.

Victoria Blue (VB) Staining

After deparaffinization and rehydration, the sections were incubated in Victoria blue solution for 1 h and subsequently placed in 95% alcohol for 10 s, then washing in distilled water for 2 min. They were next placed in Van Gieson for staining for 2–3 min and were then dehydrated with 95% alcohol and absolute alcohol. Finally, the slides were mounted and microscopically examined.

Oil Red O Staining

Frozen sections were fixed with formaldehyde-calcium for 10 min, washed with distilled water, and stained with Oil Red O for 10 min. They were then separated with 60% isopropanol and counterstained with Mayer hematoxylin. Finally, the sections were placed in water to make them blue for 1–3 min and mounted with glycerin-gelatin.

Immunofluorescence (IF) Test

Frozen sections of fresh blood vessels were taken and fixed with 4% paraformaldehyde, followed by incubation with primary antibody CD177 (the neutrophil marker for human [14], 1:200, ab256510, Abcam, USA), or Ly6G (a protein of similar structure as CD177 for mice [15], 1:200, ab25377, Abcam, USA), and the corresponding secondary antibody. The nuclei were visualized by DAPI staining. Cells were counted by the Image-Pro Plus software analysis (Media Cybernetics Inc., USA). Approximately, 5 non-overlapping

fields of representative clusters were captured for every sample with the same conditions of light intensity and exposure time at high power field (100 μm). Total cell counts were recorded and quantified by percent (% represents positive cells of total cells).

Blood Pressure Measurement

A non-invasive tail cuff detection method was used to measure systolic blood pressure on all mice after the completion of the intervention. First, the mice were adaptively acclimated to ensure that the value truly reflects the blood pressure state of the mice. The awake mice were placed in a holder equipped with a thermostatic blanket at 37 °C, and the mice tails were passed through the air bag at the back of the holder. Then, the blood pressure was detected by the software of the detection system and performed three times in each round; the deviation of the measured values did not exceed 20 mmHg.

Co-culture of Neutrophils and Mouse Aortic Vascular Smooth Muscle Cells

Neutrophils and mouse aortic vascular smooth muscle cells co-culture system was constructed (diagrammatic sketch shown in Fig. 6c). Neutrophils were isolated from murine bone marrow and then cultured in transwell chamber; the pore size of fibrous membrane is 8 μm. Mouse aortic vascular smooth muscle cells (MOVAS cell line) were cultured in the lower layer of the chamber.

A brief description of neutrophil separation was as follows. AD mice were euthanized and separated from tibia and femur. After soaking in 75% alcohol for 5 min, both ends of the bone marrow were removed. The bone marrow was rinsed with 1640 medium containing 10% FBS (Gibco, Grand Island, USA) and filtered with 70 μm nylon screen, and cells were collected by centrifugation. Bone marrow neutrophil separation reagent kit (P8550, solarbio, China) was used to isolate neutrophils.

MOVAS cell line was purchased from Fenghui Biotechnology (CL0710, Fenghui Biotechnology, China), cultured with DMEM containing 10% FBS and high glucose (Gibco, Grand Island, USA) to the second generation for experiment.

After co-culture for 48 h, the density of MOVAS cells was microscopically examined. Apoptosis of MOVAS cells was detected through fluorescein annexin V-FITC/PI double labeling, and MMP9 expression was detected by ELISA in the cell supernatant.

Apoptosis Detection

Paraffin sections of aortic vascular tissue were deparaffinized and rehydrated and then tested with the terminal deoxynucleotidyl transferase dUTP nick end labeling (TUNEL) reaction. Take appropriate amount of TDT enzyme, dUTP, and buffer in the TUNEL Assay Kit (G1507-50 T, Servicebio, China) according to the number of slices and tissue size and mixed at 1:5:50 ratio. Prepare this reaction solution according to demand before use. Add this mixture to objective tissue placed in a flat wet box, incubated at 37 ℃ for 1 h, followed by DAB developed. Nucleus stained with hematoxylin was blue. The positive apoptosis cells developed by DAB reagent had brown-yellow nucleus.

The adhering MOVAS cells were trypsinized and submitted to staining with Annexin V-FITC Apoptosis Detection Kit (C1062L, Beyotime, China), and screened on a CytoFLEX flow cytometry (Bechman coulter Inc. USA).

Enzyme-Linked Immunosorbent Assay (ELISA)

The vascular interstitial fluids of animals and the cell co-culture supernatants were to be examined the levels of MMP9 by using ELISA kit (ab253227, Abcam, USA) according to the manufacturer's instructions. Briefly, 100 μL of each sample or standard dilution was added to each well. Following incubation with unbound biotin-conjugated secondary antibodies, streptavidin labeled with horseradish peroxidase (HRP) was added to bind the biotin-labeled antibody. Tetramethylbenzidine substrate solution was used for visualization. Optical density was measured at 450 nm.

Cell Communication Analysis

To study the interactions between the major cell types in AD tissues, the Zerocode cell communication platform is used to visually infer cell–cell communication from combined expression of multi-subunit receptor-ligand complexes based on CellPhoneDB database [16, 17]; the redder the color, the higher the display value, indicating stronger interactions between cells.

Statistical Analysis

The SPSS19.0 statistical software was used for statistical analysis. Continuous variables are expressed as mean ± standard deviation (mean ± SD). After ascertaining normality of distribution via the Shapiro-Wilk test, the independent sample *t*-test was used for comparison between two groups, and one-way analysis of variance (ANOVA) followed by Scheffé post hoc test was used for comparison between multiple groups. For incidence, the difference of values was calculated using a chi-square test and pairwise comparisons of incidences were performed using a Tukey's HSD multiple comparisons test. A p-value of < 0.05 was considered to be statistically significant.

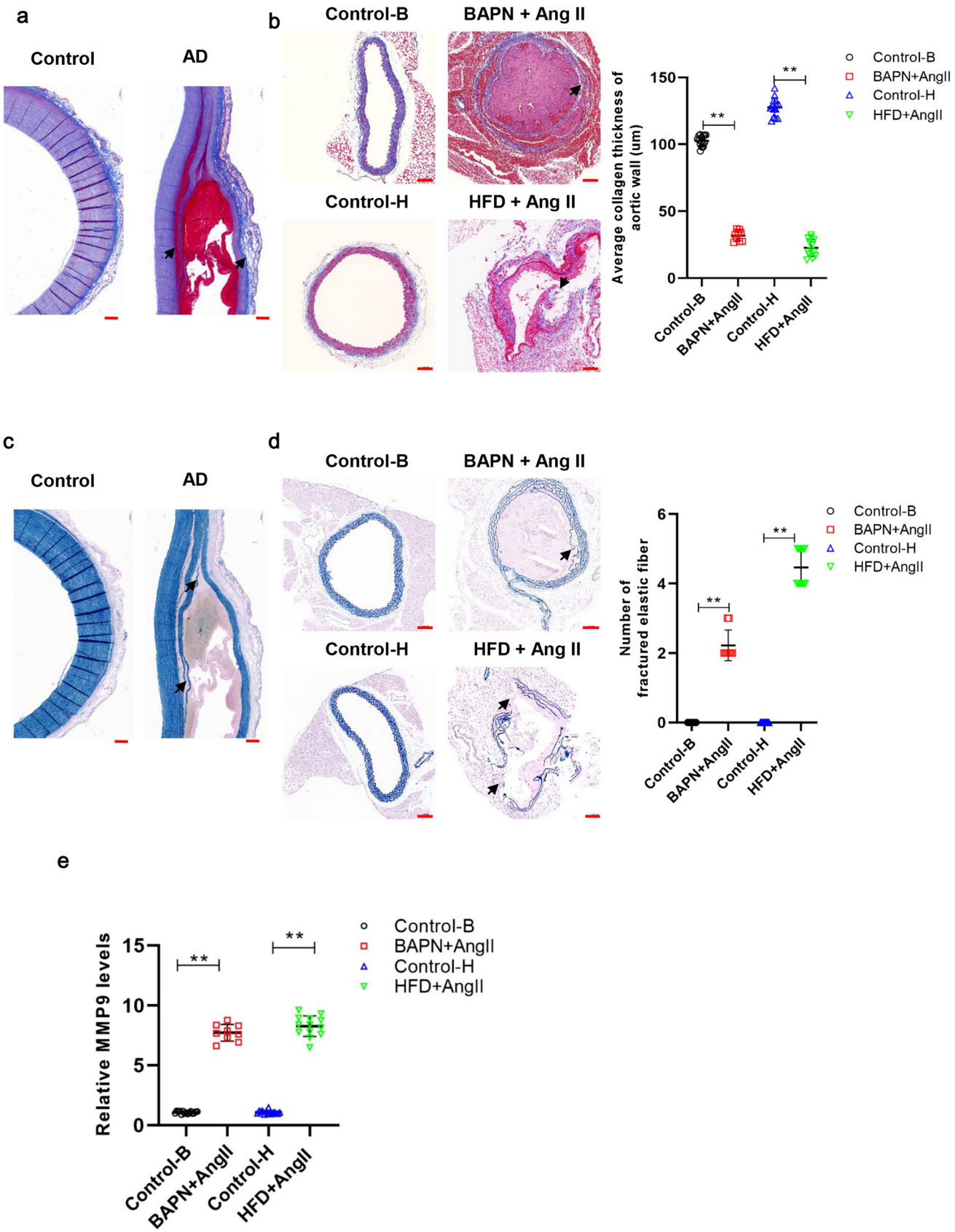
a
Control
AD
b
Control-B
BAPN + Ang II
Control-H
HFD + Ang II
Average collagen thickness of aortic wall (um)
150
100
50
0
**
**
Control-B
BAPN+AngII
Control-H
HFD+AngII
c
Control
AD
d
Control-B
BAPN + Ang II
Control-H
HFD + Ang II
Number of fractured elastic fiber
6
4
2
0
**
**
Control-B
BAPN+AngII
Control-H
HFD+AngII
e
Relative MMP9 levels
15
10
5
0
**
**
Control-B
BAPN+AngII
Control-H
HFD+AngII

◂**Fig. 2** Detection of histopathological changes of aorta in the two kinds of AD models in mice. **a** Masson staining to show collagen in the dissection (AD) and non-dissection (Control) parts of blood vessels of AD patient. The vascular wall collagen of the false lumen inpatients was structurally broken and significantly reduced (arrows). Scale bar, 500 μm. **b** Masson staining to show the pseudo-lumen vascular wall collagen was structurally broken and missing (arrows) in the two intervention groups of mice, while the collagen layers of the blood vessels in corresponding control mice were thicker, the structures were complete, continuous, and not missing. Scale bars, 100 μm. $^{**}p < 0.01$. **c** Victoria blue (VB) staining to show the elastic fiber layers in the AD patient were structurally broken and thinner (arrows). Scale bar, 500 μm. **d** VB staining to show the pseudo-lumen vascular wall elastic fiber layers were structurally broken and missing (arrows) in the intervention groups, while the elastic fibers of the blood vessels in control mice presented a filamentous, multilayer compact distribution. Scale bar 100 μm. $^{**}p < 0.01$. **e** The relative MMP9 expression measured by using ELISA in the vascular interstitial fluids of animals. $^{**}p < 0.01$. Control-B: control group of "BAPN + AngII" group; Control-H: control group of "HFD + AngII" group; $n = 15$

Results

Both Models Induced AD in Mice

The strategy for the construction of the two AD models is outlined in Fig. 1a. Following the completion of the interventions, the heart, aorta, and kidney tissues of the mice were stripped and used to calculate the incidence of dissection. We observed both "BAPN + AngII" and "HFD + AngII" intervention groups could induce AD (Fig. 1b).

To verify whether the murine models can simulate human AD, we examined and compared changes in vessel morphology in human and mice. HE staining showed that there were large amounts of red blood cells infiltrating between the media and intima in the blood vessels of AD patients, forming a false cavity, whereas there was no false lumen in the non-sandwich areas and the structures were complete and compact (Fig. 1c). We confirmed that both intervention models could simulate the structural changes in patients with AD (Fig. 1d). In addition to the large vascular lumens (blue arrow) in the two intervention groups, small false lumen (green arrow) appeared in the blood vessels of the mice that formed dissections and large amounts of red blood cells entered the false lumen. The above results illustrate that these two treatments can be used to construct AD models.

Both Models Caused Histopathological Alterations of Aorta in Mice

To further investigate the effects of two kinds of interventions on the morphology of the aorta, histological alterations were observed in both murine models and AD patients. AD pathogenesis occurs due to collagen deposition and elastin degradation, along with the dysfunctions of the elastic lamina layer of the aorta wall.

Masson staining showed that collagen was broken and missing around the blood vessel wall in the dissected part of the patient, but the collagen distributed in the non-dissected part was uniform and complete (Fig. 2a). Similarly, the vascular wall of the AD mice of the two intervention groups became thinner, collagen fibers were reduced, and some parts were missing and discontinuous; these structural changes may lead to infiltration of inflammatory cells. In the control mice, the collagen layers were thicker and the structures were complete, continuous, and not missing (Fig. 2b).

VB staining revealed that the elastic fibers of the vessel wall at the dissection site of AD patients had been obviously destroyed, which were mainly reflected in the lack of structure and reduction of components (Fig. 2c). Similar changes also occur in animal models, the elastic fibers suffered different degrees of damages, discontinuous fractures appeared, and the elastic fibers were relatively loose in AD mice (Fig. 2d). However, these changes were not detected in the vascular tissues of the control mice.

The degradation of the extracellular matrix (ECM) is the main reason for the pathological changes in aortic mechanical properties. The release of matrix metalloproteinases (MMPs) can lead to excessive ECM degradation. Upregulation of MMPs, particularly the MMP9, has been identified as a key event during AD progression [18]. Since the changes in collagen and elastic fibers of the ECM in AD mice were particularly noticeable, we determined MMP9 expression using ELISA in the two murine models. The significant increase of MMP9 expression was detected in both two intervention groups (Fig. 2e). This result suggests that both treatments can affect the expression of MMP9, thereby destroying ECM stability and promoting AD development.

The Two Models Imitated Different Classifications of AD

Firstly, we evaluated the incidence and mortality of AD in the two models (Table 1). The occurrence of AD in each group was as follows: 13 of the 15 mice in the "HFD + AngII" group developed AD, and the incidence of dissection reached 86.67%. The incidence of dissection in the "BAPN + AngII" group was lower: 9 of 15 mice developed AD, with an incidence rate of up to 60% (Fig. 3a). No mouse died in the control group; however, death was recorded in both the "HFD + AngII" and "BAPN + AngII" groups. The cause of death was hemorrhage caused by the rupture from the dissection. Two mice in the "HFD + AngII" group died due to AD rupture after AngII micropump implantation in the 4th week; the mortality rate was 13.33%. In the "BAPN + AngII" group, five mice died due to ruptured AD, one mouse died in the 3rd week after BAPN

Table 1 Comparison of two mouse AD models

	Control-B ($n=15$)	BAPN + AngII ($n=15$)	Control-H ($n=15$)	High-fat + AngII ($n=15$)
Mortality rate	0	5/15 (33.33%)	0	2/15 (13.33%)
Incidence of AD	0	9/15 (60%)	0	13/15 (86.67%)
Type of AD				
DeBakey type I		2/9 (22.22%)		3/13 (23.08%)
DeBakey type II		2/9 (22.22%)		4/13 (30.77%)
DeBakey type III		5/9 (55.56%)		6/13 (46.15%)
or				
Stanford type A		4/9 (44.44%)		7/13 (53.85%)
Stanford type B		5/9 (55.56%)		6/13 (46.15%)

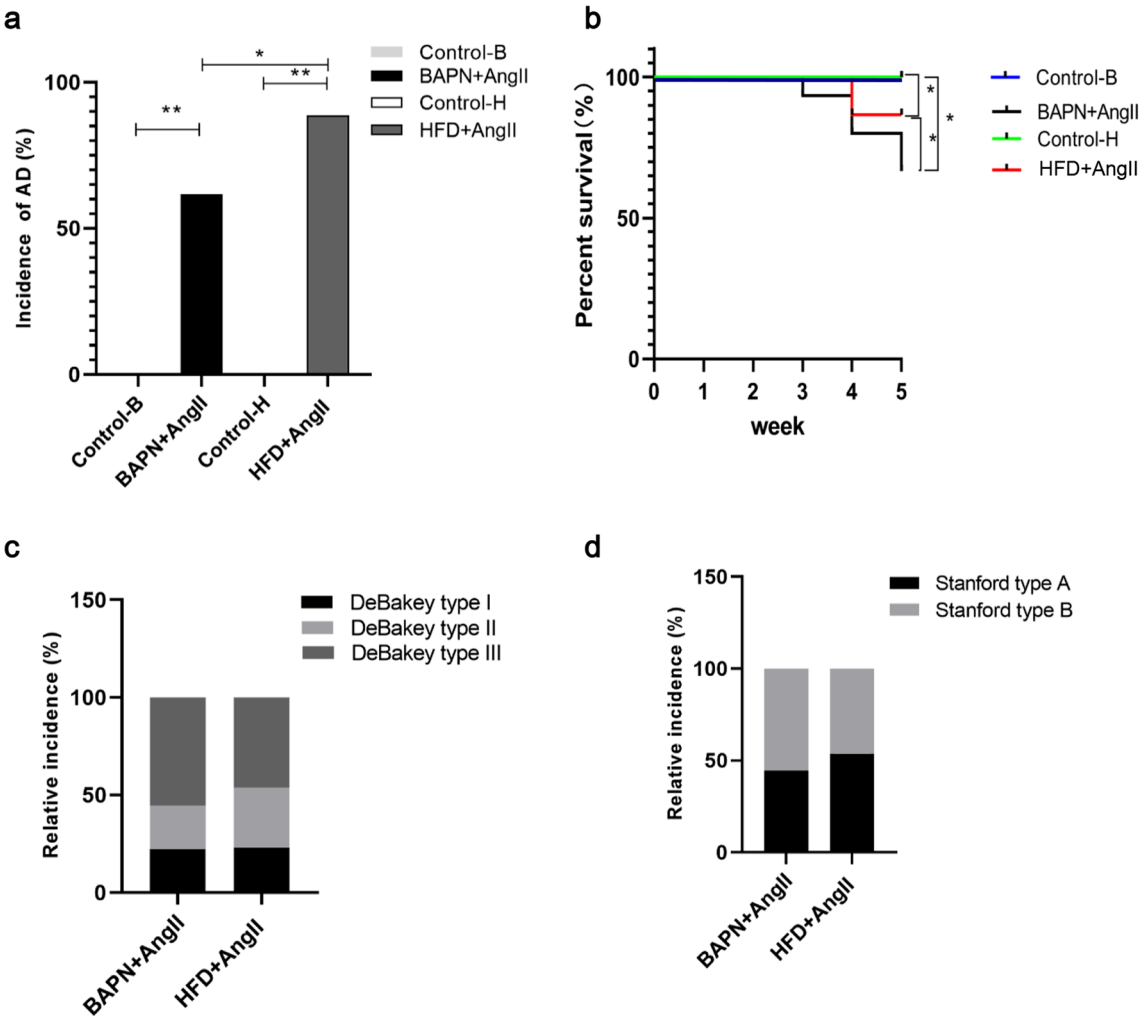

Fig. 3 Evaluation of AD incidence, mortality and AD classifications in the two kinds of murine models. **a** The incidence of AD in two kinds of murine models. The difference of incidence values was calculated using a chi-square test and pairwise comparisons of incidences were performed using a Tukey's HSD multiple comparisons test. *$p<0.05$. **b** The Kaplan-Meier curve survival analysis between different groups. No mice died in the two control groups, but some mice died in both and "BAPN + AngII" group and "HFD + AngII" group. *$p<0.05$. **c**–**d** The relative incidence of different AD types in the two intervention groups according to DeBakey classification (**c**) and Stanford classification (**d**) separately. Control-B: control group of "BAPN + AngII" group; Control-H: control group of "HFD + AngII" group; $n=15$

intervention, two died in the 4th week, and two died 72 h after the implantation of the AngII micropump. The mortality rate was 33.33%. Figure 3b shows the Kaplan-Meier curve survival analysis of the different groups.

Aortic dissections in patients commonly involve the ascending, thoracic (descending aorta in the chest), and abdominal aorta. AD can be subdivided into type I, II, and III by Debakey classification according to the location of the initial tear of AD and the range of tear accumulation [12]. The simpler Stanford Classification has become well established recently based on the surgery's demand [13]. Dissection of Stanford type A is generally more common in other regions and is seen in two-thirds of the clinical cases collected from the IRAD series. As shown in Table 1 and Fig. 3c–d, "BAPN + AngII" intervention caused most of the mice to develop AD in thoracic aorta and abdominal aorta; in other words, this treatment mainly stimulated AD belonging to the DeBakey type III or Stanford type B, whereas dissection induced in the "HFD + AngII" group involving the ascending aorta, belonged to DeBakey type I–II or Stanford type A. We speculate that may be because atherosclerosis often occurs in the coronary artery, which is a branch of the ascending aorta. In this aspect, our model is more suitable for simulating a type consistent with actual clinical conditions. Although there was no statistical difference, it is undeniable that our sample size is not very large; further validation and optimization of this model should be conducted.

Induction of AD by the Combination of HFD and AngII Is Closely Related with Atherosclerotic Lesions of Arteries

Body weight measurement provides a general understanding of mice in a noninvasive manner. There was no difference in the body weight of mice in "BAPN + AngII" group and "Control-B" group. And due to the short time of AngII treatment, there was no significant change before and after the injection (Fig. 4a). However, the body weight of the mice in the "HFD + AngII" group gradually increased, but dropped a little after injection of AngII (Fig. 4b).

The most prominent risk factor hypertension can cause increased pressure on the aortic wall, which can trigger the development of an intimal tear. We measured the systolic blood pressure of mice after the experimental intervention. Blood pressure in each group showed a normal distribution. As shown in Fig. 4c, the systolic pressure of both "BAPN + AngII" and "HFD + AngII" intervention groups was indeed much higher than that of their corresponding control groups, confirming that hypertension really played an important role in AD progression.

Dyslipidemia and atherosclerosis have become common diseases endangering health, and the related AD incidence has increased significantly. We used Oil Red O staining to quantify the atherosclerotic burden in murine tissues. Obvious plaques with lipid deposition were seen only in "HFD + AngII" intervention group, which morphologically reproduced AD features associated with atherosclerosis. In contrast, lipid deposition was almost undetectable in the other groups (Fig. 4d). This indicates that our combination treatment can simulate atherosclerotic lesions of arteries in AD, which is more clinically relevant.

Neutrophils Significantly Infiltrated into Aortic Wall Tissue in the AD Model Induced by Combination of HFD and AngII

Inflammation is closely related to the occurrence and development of AD. Recently, increasing evidence has shown that neutrophils contribute to AD pathogenesis [19], or suggested the predictive value in diagnosis and prognosis [20]. Accordingly, we used CD177 (a human neutrophil marker) to label the patient's specimen and found a large number of neutrophils accumulated in the dissected tissue of the patient (Fig. 5a). The similar IF results confirmed neutrophil (labeled with a murine neutrophil marker Ly6G) infiltration in the blood vessels of AD mice (Fig. 5b). Additionally, the degree of neutrophil accumulation in the "HFD + AngII" group was more serious than that in co-administration of BAPN and AngII, suggesting a more important role of neutrophils during the formation of atherosclerosis-associated AD.

Moreover, we investigated the interactions between cells in AD tissues by Zerocode communication platform based on CellPhoneDB database. Figure 5c shows that the color of square covered neutrophils and vascular smooth muscle cells (SMC) was the reddest, indicating the strongest association between these two kinds of cells.

Neutrophils Induced Apoptosis of Aortic Vascular Smooth Muscle Cells

VSMCs are the predominant cell type within the aortic wall and essential for ECM regeneration, the loss of VSMCs can weaken the aortic wall and limits matrix repair capacity, and dysfunction of VSMCs can promote AD development. Various mechanisms to induce the switch of VSMCs to a more senescent phenotype with high susceptibility to apoptosis were reported. TUNEL staining showed that the apoptosis rate of VSMCs was markedly higher in dissection section from human sample (Fig. 6a). A similar result existed in the two murine models, and more serious in the "HFD + AngII" group (Fig. 6b).

We then co-cultured the neutrophils and mouse aortic vascular smooth muscle cells (MOVAS) in an in vitro experiment system (Fig. 6c). After 48 h, we found the amount of VSMCs decreased substantially (Fig. 6d), probably due to an

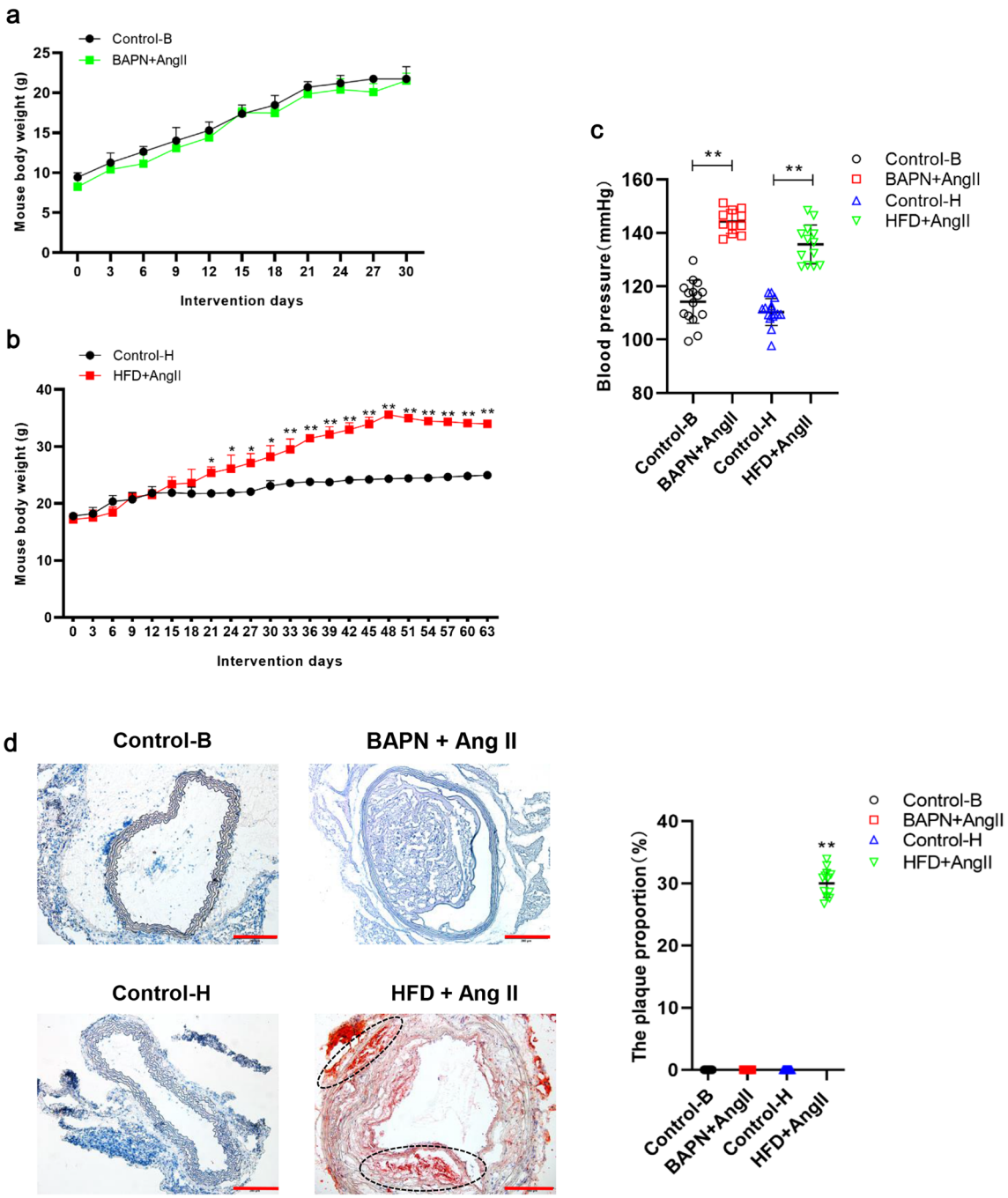

Fig. 4 The effect of the two kinds of intervention on body weight, blood pressure, and arterial plaque. **a**–**b** The changes of weight in "BAPN + AngII" group (**a**) and "HFD + AngII" group (**b**), compared with corresponding control groups. Mice were weighed and recorded every 3 days. $*p < 0.05$, $**p < 0.01$. **c** The systolic blood pressure of mice in different groups after intervention measured by the non-invasive tail cuff detection method. $**p < 0.01$. **d** Representative Oil Red O staining to quantify atherosclerotic burden in different groups of mice (circle showing lipid deposition), $**p < 0.01$ vs other groups. Scale bars, 200 μm. Control-B: control group of "BAPN + AngII" group; Control-H: control group of "HFD + AngII" group; $n = 15$

increased apoptosis (Fig. 6e). A high expression of MMP9 was also observed in the cell supernatant of co-culture system (Fig. 6f). Above results suggest the effect of neutrophils on VSMCs may play a greater role in the development of atherosclerosis-related AD.

Discussion

Animal modeling is a prerequisite for the clinical transfer of new therapies, such as identification of biomarkers, advances in modern imaging technology for early diagnosis

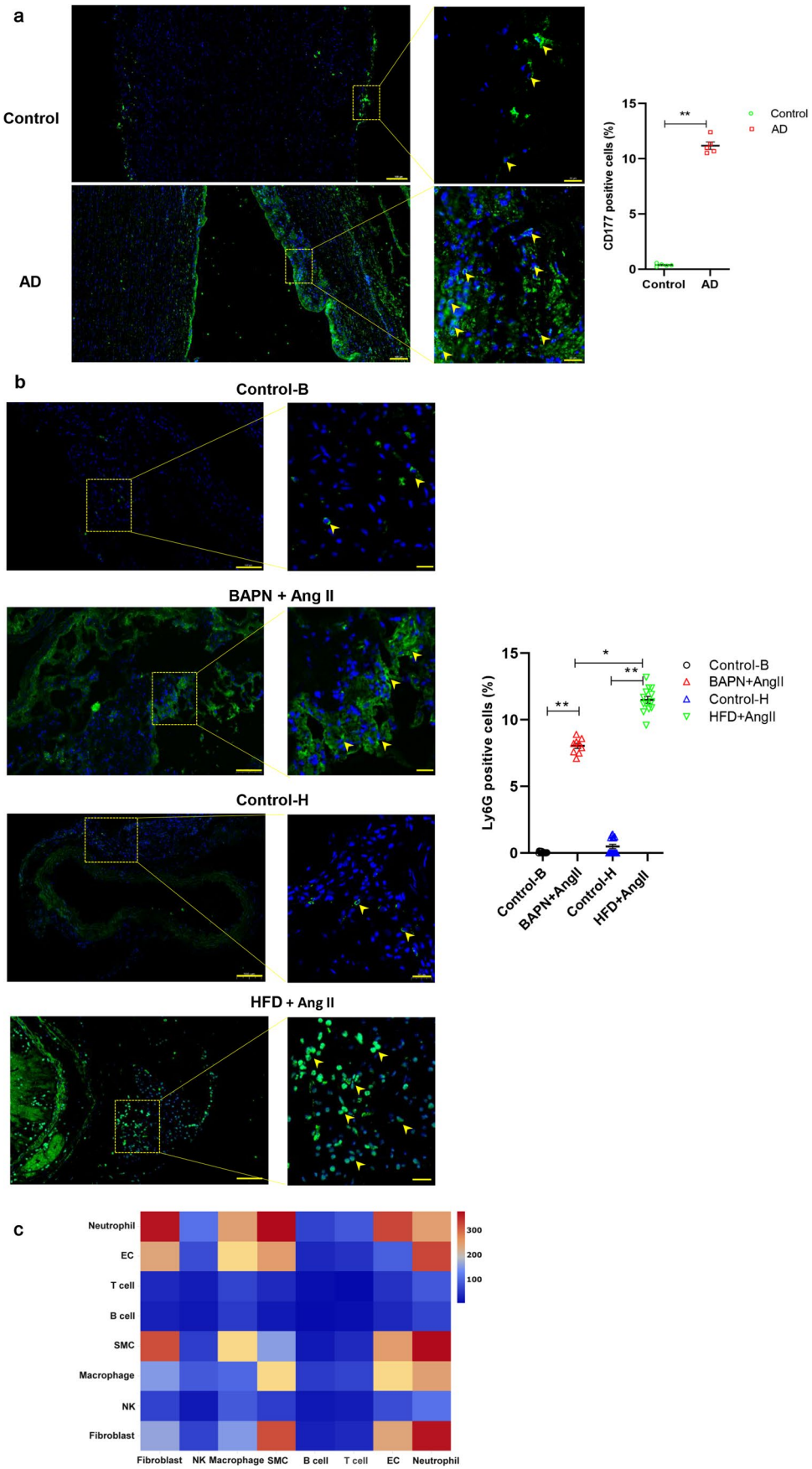

Fig. 5 Assay of neutrophil infiltration in the aorta tissues of AD patients and the murine AD models. **a** Neutrophils stained with CD177 antibody (green) in human specimens, AD: dissection tissue, Control: non-dissection tissue. $^{**}p < 0.01$. **b** Neutrophils stained with Ly6G antibody (green) in the aortic vessels of mice in different groups. Control-B: control group of "BAPN + AngII" group; Control-H: control group of "HFD + AngII" group; $n = 15$. The nuclei were visualized by DAPI staining (blue). Scale bars, 100 μm or 20 μm. The Image-Pro Plus software was used for measurement. Statistical data revealed relative percentage of positive staining cells. $^{*}p < 0.05$, $^{**}p < 0.01$. **c** Cell communication analysis displayed the interactions between the major cell types in AD tissues by the Zerocode cell communication platform based on CellPhoneDB database; the redder the color, the higher the display value, indicating stronger interactions between cells

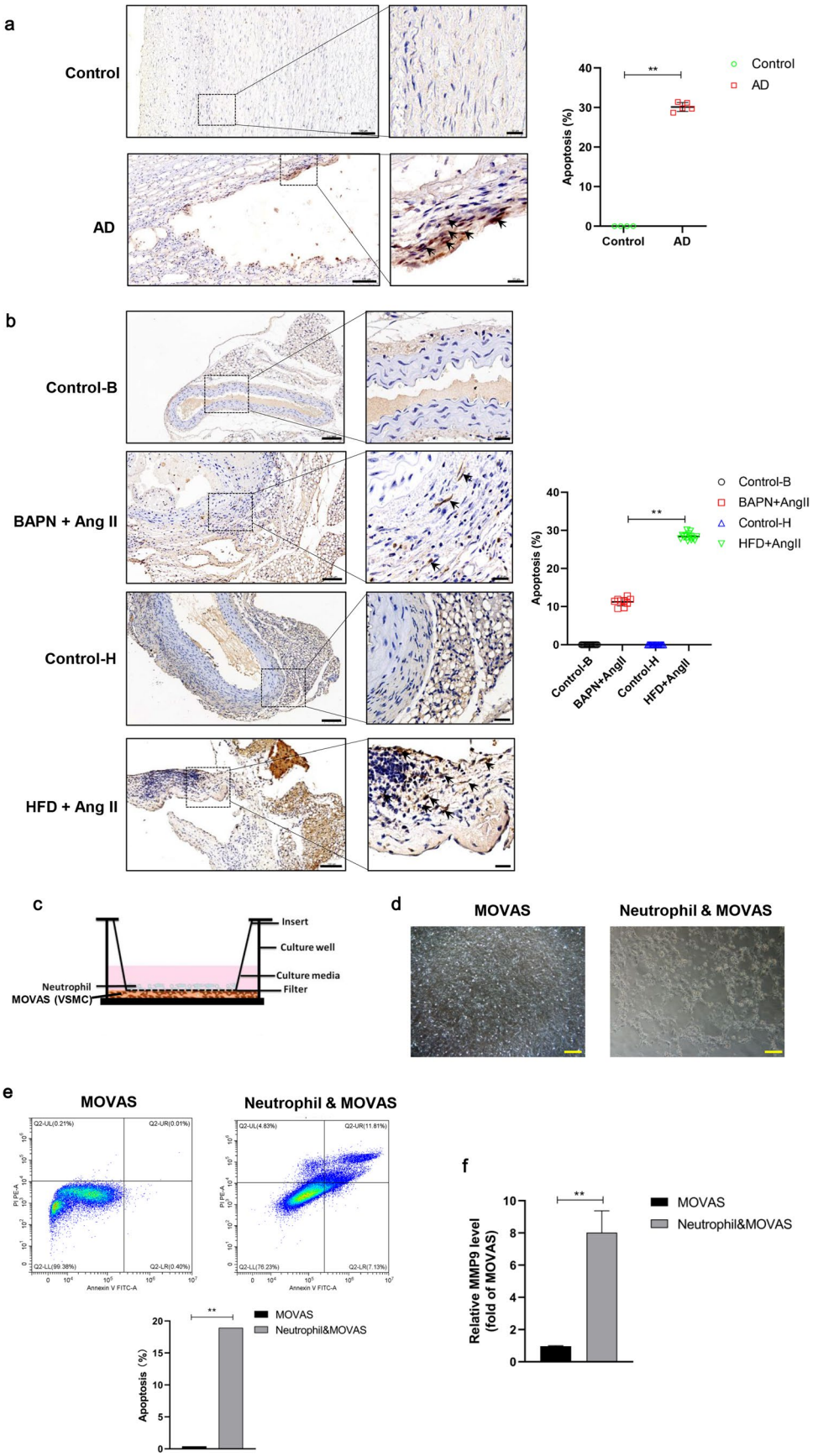

Fig. 6 Investigation of apoptosis of aortic vascular smooth muscle cells. **a** The apoptosis level of aortic vascular tissue cells tested by TUNEL method in in human specimens, AD: dissection tissue, Control: non-dissection tissue. $^{**}p < 0.01$. **b** The apoptosis level of the aortic vessels of mice in different groups tested by TUNEL method, Control-B: control group of "BAPN + AngII" group; Control-H: control group of "HFD + AngII" group; $n = 15$. Scale bars, 100 μm or 20 μm. $^{**}p < 0.01$. **c** In vitro experiment of co-culture system model between neutrophils and mouse smooth muscle cells. Neutrophils were isolated from mouse bone marrow and then cultured in transwell chamber; mouse aortic vascular smooth muscle cells (MOVAS cell line) were cultured in the lower layer of the chamber. **d** Microscopic observation of neutrophils and MOVAS cells after 48-h co-culture. Scale bars, 100 μm. **e** Detection of apoptosis of MOVAS cells through fluorescein annexin V-FITC/PI double labeling after 48-h co-culture. $^{**}p < 0.01$. **f** Relative MMP9 level in the cell supernatant after 48-h co-culture detected by ELISA. $^{**}p < 0.01$

and guiding treatment strategies, and improvement of stent-graft technology for broader endovascular treatment applications. Different kinds of AD animal models have been established in previous studies; nevertheless, each model has its advantages and disadvantages.

Based on its relatively low price, easy-to-control genetic background, and convenient intervention methods, the murine AD model is more convenient and economical than other models. Recent murine AD models mainly consist of two major categories. One is induced by transgenic technology that mimics inherited connective tissue disorder-associated AD [21, 22]. However, the occurrence of AD in genetically modified models is low and requires a combination of surgical intervention and drug administration to effectively induce AD [23, 24]. The other, which is currently commonly used, is induced by chemicals, such as AngII and BAPN, which simulate hypertension-induced AD. AngII, the principal effector of the renin–angiotensin–aldosterone system [25], mainly influences hemodynamics, such as increasing blood pressure and shearing force of blood flow in the vessel wall to cause AD [26]. BAPN is a potent and irreversible inhibitor of lysyl oxidase (Lox), which can break down and degrade the cross-links between elastin and collagen by inhibiting Lox [27], resulting in decreased vascular wall toughness and increased fragility[28]. However, using either AngII or BAPN alone, the incidence of AD is low, and AD induced by BAPN also appear to be reduced with age, whereas the combination of BAPN and AngII can increase the occurrence of AD but with significantly increased uncontrollable death [29, 30], rendering it unsuitable for use in subsequent studies.

Advanced age, male gender, long-term history of arterial hypertension, and the presence of connective tissue disorders such as Marfan syndrome confer the greatest population attributable risk [31]. In recent years, the incidence of AD complicated by atherosclerosis has increased. Although much research has been conducted to determine correlations between atherosclerosis and hypertension [32, 33], the interrelated and mutually potentiating molecular mechanisms have not been clearly elucidated. In general, in relation to dyslipidemia, high blood pressure may act as a trigger for atherosclerotic lesions and its devastating consequences [34]; the incidence of atherosclerosis in hypertensive patients is significantly higher than that in the general population. Arterial stenosis caused by atherosclerotic plaques can also aggravate hypertension simultaneously. Furthermore, endothelial damage and abnormal function of VSMCs have been implicated in both atherosclerosis and hypertension [35], which are also key pathological features of AD. Atherosclerosis and hypertension create a self-perpetuating vicious cycle that accelerates AD progression. Thus, we want to set up a stable effective model with consideration of multiple risk factors.

ApoE-/- mice have traditionally been placed on HFD for atherosclerosis research [36, 37]. However, different concentrations of AngII have different effects on blood vessels in mice of different ages. A previous research determined AngII-induced hypertension would accelerate the development of atherosclerotic lesions by using AngII infusion with HFD together in young mice [38]. There has been other prior reports in the literature (PMID 20177736) that in ApoE-/- mice both HFD and AngII independently were able to induce aneurysms in mature age mice (but occurrence of dissections was not documented) [39]. In our preliminary experiment, after 9 weeks of HFD on ApoE-/- mice, we actually only found in HFD group that the lipid plaques were deposited in the artery wall of mice, collagen and elastic fibers became loose, but no dissection was generated (Supplementary Fig. 1). These results demonstrate that a simple high fat-diet alone without AngII treatment could not induce AD effectively, which is consistent with the above reports. Thus, it can be seen that AngII treatment for 2nd-hit is very necessary for inducing AD in mice. While we adopted new construction strategies to establish a novel model of AD, we promoted the development of atherosclerosis in mature mice with a HFD firstly, and combined with AngII treatment subsequently to facilitate the formation of dissection. It is precisely because of these differences including mice age, construction strategies, and dose of AngII that different models resulted in different diseases.

We compared and analyzed this model with the traditional chemical induction model; the pathogenesis of AD simulated by the two modeling methods is quite different. The model based on traditional induction of BAPN and AngII, mimicking the pathological process of AD caused by hypertension, is closer to the condition that young people suffer from stress damage. But our novel model combined with HFD and AngII considering multiple risk factors is more capable of simulating clinical atherosclerosis-related AD.

Admittedly, there are some limitations of our current study. Firstly, mouse strain, age of assessment, and duration of AngII treatment differences make it difficult to directly claim that one model has better mortality and higher AD rates. Our method requires a much longer modeling time compared to previous chemical induction, but to a reasonable extent, our model may be a long-term useful tool for more in-depth investigation of AD mechanisms and thus be beneficial for therapeutic developments. Also, another limitation of the current study is the lack of appropriate control groups. In this study, we mainly focus on comparing the different AD incidence and characteristics between the two intervention models: HFD (a chronic vascular lesion inducing factor) and BAPN (a vascular stress treatment). Therefore, for the "HFD + AngII" intervention group, normal mice served as the control. It has

been reported that the incidence of AD in animal models was very low when using AngII alone [8], so we have not set AngII-loaded pump and control diet as a control. But in the experiment, we found that the food intake of the "HFD + AngII" group was evidently less than that of the normal control group during the chronic treatment of AngII. Difference of food intake might limit the interpretation of the results. Furthermore, the addition of AngII is a determinant for a model of AD based on the results shown in Supplementary Fig. 1. Thus, the most appropriate "intermediate" control to this 2nd-hit model will be a comparison with age-matched mice on HFD without the AngII.

Previous investigations indicate inflammatory immune response of the aorta is the key pathophysiological basis for the process of cardiovascular diseases. Inflammation is also the bridge between hypertension and atherosclerosis [40], thus can play a crucial role during the remodeling process of the aortic wall structure in the development of AD [41]. Neutrophils not only are inflammatory cells, but also participate in the initiation of plaque development, and further release inflammatory factors and MMP 2/9, to promote the inflammatory reaction process of the outer membrane and eventually leading to the progress and rupture of the dissection. Additionally, the neutrophil-to-lymphocyte ratio (NLR) is a good inflammatory marker because of fast detection and low price. NLR has recently been reported to serve as diagnosis and prognosis assessment in AD [42–44]. In this study, we observed that the degree of neutrophil infiltration was more serious in the "HFD + AngII" group.

Degradation of ECM causing AD is a "terminal" event, modulated by genetic background, hemodynamic strain, or cellular events. The loss of VSMCs in the medial layer of the aortic wall due to apoptosis is an early hallmark of development and progression of aortic aneurysms and dissections. The infiltration of different inflammatory cell types affects VSMC functions, such as macrophages and natural killer T (NKT) cells [45]. A research team from Germany reported that neutrophils aggravate atherosclerosis by inducing death of VSMCs [46]. In our present study, we showed that excessive apoptosis of VSMCs, along with neutrophil infiltration, was present in AD samples from both human and two murine models. Furthermore, the level was more serious in our novel "HFD + AngII" model. Cell communication analysis displayed the strongest association between VSMCs and neutrophils, and in vitro co-culture experiment also showed neutrophils might induce VSMC apoptosis. These results suggest the effect of neutrophils on VSMCs may play a more important role in the development of atherosclerosis-related AD. Further in-depth research is needed to be performed in the future.

Conclusions

Advanced age, longer hypertension history, and some combined vascular atherosclerosis, which are associated with medial degeneration, are considered the most common predisposing factors for AD. Therefore, our "HFD + AngII" model is more perfectly suited for exploring the underlying mechanisms of atherosclerosis-related AD based on chronic vasculopathy in clinic than traditional chemically induced model.

Supplementary Information The online version contains supplementary material available at https://doi.org/10.1007/s12265-023-10408-3.

Acknowledgements We would like to thank Editage (www.editage.cn) for English language editing.

Funding The present study was supported by the grants from National Natural Science Foundation of China (No. 81670407 and No. 82201941), Army Foundation of PLA (20WQ004) and Talents Support Project of Army Medical University (No.410301060131).

Data Availability The data underlying this article cannot be shared due to the privacy of the patient. The data will be shared on reasonable request to corresponding author.

Declarations

Conflict of Interest The authors declare no competing interests.

References

1. Nienaber CA, Clough RE, Sakalihasan N, Suzuki T, Gibbs R, Mussa F, Jenkins MP, Thompson MM, Evangelista A, Yeh JS, et al. Aortic dissection. Nat Rev Dis Primers. 2016;2:16053.
2. Golledge J, Eagle KA. Acute aortic dissection. Lancet. 2008;372(9632):55–66.
3. Evangelista A, Isselbacher EM, Bossone E, Gleason TG, Eusanio MD, Sechtem U, Ehrlich MP, Trimarchi S, Braverman AC, Myrmel T, et al. Insights from the international registry of acute aortic dissection: a 20-year experience of collaborative clinical research. Circulation. 2018;137(17):1846–60.
4. Komatsu S, Takahashi S, Yutani C, Ohara T, Takewa M, Hirayama A, Kodama K. Spontaneous ruptured aortic plaque and injuries: insights for aging and acute aortic syndrome from non-obstructive general angioscopy. J Cardiol. 2020;75(4):344–51.
5. Caielli P, Frigo AC, Pengo MF, Rossitto G, Maiolino G, Seccia TM, Calò LA, Miotto D, Rossi GP. Treatment of atherosclerotic renovascular hypertension: review of observational studies and a meta-analysis of randomized clinical trials. Nephrol Dial Transplant. 2015;30(4):541–53.
6. Hurtubise J, McLellan K, Durr K, Onasanya O, Nwabuko D, Ndisang JF. The different facets of dyslipidemia and hypertension in atherosclerosis. Curr Atheroscler Rep. 2016;18(12):82.
7. Erbel R, Aboyans V, Boileau C, Bossone E, Bartolomeo RD, Eggebrecht H, Evangelista A, Falk V, Frank H, Gaemperli O, et al. 2014 ESC guidelines on the diagnosis and treatment of aortic diseases: document covering acute and chronic aortic diseases of the thoracic and abdominal aorta of the adult. The

Task Force for the Diagnosis and Treatment of Aortic Diseases of the European Society of Cardiology (ESC). Eur Heart J. 2014;35(41):2873–926.
8. Jiang DS, Yi X, Zhu XH, Wei X. Experimental in vivo and ex vivo models for the study of human aortic dissection: promises and challenges. Am J Transl Res. 2016;8(12):5125–40.
9. Zheng HQ, Rong JB, Ye FM, Xu YC, Lu HS, Wang JA. Induction of thoracic aortic dissection: a mini-review of β-aminopropionitrile-related mouse models. J Zhejiang Univ Sci B. 2020;21(8):603–10.
10. Anzai A, Shimoda M, Endo J, Kohno T, Katsumata Y, Matsuhashi T, Yamamoto T, Ito K, Yan X, Shirakawa K, et al. Adventitial CXCL1/G-CSF expression in response to acute aortic dissection triggers local neutrophil recruitment and activation leading to aortic rupture. Circ Res. 2015;116(4):612–23.
11. LeMaire SA, Zhang L, Luo W, Ren P, Azares AR, Wang Y, Zhang C, Coselli JS, Shen YH. Effect of ciprofloxacin on susceptibility to aortic dissection and rupture in mice. JAMA Surg. 2018;153(9):e181804.
12. DeBakey ME, McCollum CH, Crawford ES, Morris GC Jr, Howell J, Noon GP, Lawrie G. Dissection and dissecting aneurysms of the aorta: twenty-year follow-up of five hundred twenty-seven patients treated surgically. Surgery. 1982;92(6):1118–34.
13. Crawford ES, Svensson LG, Coselli JS, Safi HJ, Hess KR. Aortic dissection and dissecting aortic aneurysms. Ann Surg. 1988;208(3):254–73.
14. Lévy Y, Wiedemann A, Hejblum BP, Durand M, Lefebvre C, Surénaud M, Lacabaratz C, Perreau M, Foucat E, Déchenaud M, et al. CD177, a specific marker of neutrophil activation, is associated with coronavirus disease 2019 severity and death. iScience. 2021;24(7):102711.
15. Zhou X, Yang L, Fan X, Zhao X, Chang N, Yang L, Li L. Neutrophil chemotaxis and NETosis in murine chronic liver injury via cannabinoid receptor 1/ Gα(i/o)/ ROS/ p38 MAPK signaling pathway. Cells. 2020;9(2):373.
16. Vento-Tormo R, Efremova M, Botting RA, Turco MY, Vento-Tormo M, Meyer KB, Park JE, Stephenson E, Polanski K, Goncalves A, et al. Single-cell reconstruction of the early maternal-fetal interface in humans. Nature. 2018;563(7731):347–53.
17. Efremova M, Vento-Tormo M, Teichmann SA, Vento-Tormo R. Cell PhoneDB: inferring cell-cell communication from combined expression of multi-subunit ligand-receptor complexes. Nat Protoc. 2020;15(4):1484–506.
18. Maguire EM, Pearce SWA, Xiao R, Oo AY, Xiao Q. Matrix metalloproteinase in abdominal aortic aneurysm and aortic dissection. Pharmaceuticals (Basel). 2019;12(3):118.
19. Sano M, Anzai J. The molecular mechanisms contributing to the pathophysiology of systemic inflammatory response after acute aortic dissection. Nihon Rinsho Meneki Gakkai Kaishi. 2016;39(2):91–5.
20. Liu H, Li D, Jia Y, Zeng R. Predictive value of white blood cells, neutrophils, platelets, platelet to lymphocyte and neutrophil to lymphocyte ratios in patients with acute aortic dissection. Braz J Cardiovasc Surg. 2020;35(6):1031–3.
21. Emrich FC, Okamura H, Dalal AR, Penov K, Merk DR, Raaz U, Hennigs JK, Chin JT, Miller MO, Pedroza AJ, et al. Enhanced caspase activity contributes to aortic wall remodeling and early aneurysm development in a murine model of Marfan syndrome. Arterioscler Thromb Vasc Biol. 2015;35(1):146–54.
22. Smith LB, Hadoke PW, Dyer E, Denvir MA, Brownstein D, Miller E, Nelson N, Wells S, Cheeseman M, Greenfield A. Haploinsufficiency of the murine Col3a1 locus causes aortic dissection: a novel model of the vascular type of Ehlers-Danlos syndrome. Cardiovasc Res. 2011;90(1):182–90.
23. Faugeroux J, Nematalla H, Li W, Clement M, Robidel E, Frank M, Curis E, Ait-Oufella H, Caligiuri G, Nicoletti A, et al. Angiotensin II promotes thoracic aortic dissections and ruptures in Col3a1 haploinsufficient mice. Hypertension. 2013;62(1):203–8.
24. Matt P, Huso DL, Habashi J, Holm T, Doyle J, Schoenhoff F, Liu G, Black J, Van Eyk JE, Dietz HC. Murine model of surgically induced acute aortic dissection type A. J Thorac Cardiovasc Surg. 2010;139(4):1041–7.
25. Paz Ocaranza M, Riquelme JA, García L, Jalil JE, Chiong M, Santos RAS, Lavandero S. Counter-regulatory renin-angiotensin system in cardiovascular disease. Nat Rev Cardiol. 2020;17(2):116–29.
26. Qin Z. Newly developed angiotensin II-infused experimental models in vascular biology. Regul Pept. 2008;150(1–3):1–6.
27. Brüel A, Ortoft G, Oxlund H. Inhibition of cross-links in collagen is associated with reduced stiffness of the aorta in young rats. Atherosclerosis. 1998;140(1):135–45.
28. Li JS, Li HY, Wang L, Zhang L, Jing ZP. Comparison of β-aminopropionitrile-induced aortic dissection model in rats by different administration and dosage. Vascular. 2013;21(5):287–92.
29. Qi X, Wang F, Chun C, Saldarriaga L, Jiang Z, Pruitt EY, Arnaoutakis GJ, Upchurch GR, Jr., Jiang Z. A validated mouse model capable of recapitulating the protective effects of female sex hormones on ascending aortic aneurysms and dissections (AADs). 2020;8(22):e14631.
30. Ren W, Liu Y, Wang X, Jia L, Piao C, Lan F, Du J. β-Aminopropionitrile monofumarate induces thoracic aortic dissection in C57BL/6 mice. Sci Rep. 2016;6:28149.
31. Gawinecka J, Schönrath F, von Eckardstein A. Acute aortic dissection: pathogenesis, risk factors and diagnosis. Swiss Med Wkly. 2017;147: w14489.
32. Shimizu Y, Kawashiri SY, Kiyoura K, Nobusue K, Yamanashi H, Nagata Y, Maeda T. Gamma-glutamyl transpeptidase (γ-GTP) has an ambivalent association with hypertension and atherosclerosis among elderly Japanese men: a cross-sectional study. Environ Health Prev Med. 2019;24(1):69.
33. Ning B, Chen Y, Waqar AB, Yan H, Shiomi M, Zhang J, Chen YE, Wang Y, Itabe H, Liang J, et al. Hypertension enhances advanced atherosclerosis and induces cardiac death in Watanabe heritable hyperlipidemic rabbits. Am J Pathol. 2018;188(12):2936–47.
34. Chobanian AV, Alexander RW. Exacerbation of atherosclerosis by hypertension. Potential mechanisms and clinical implications. Arch Intern Med. 1996;156(17):1952–6.
35. Shi J, Yang Y, Cheng A, Xu G, He F. Metabolism of vascular smooth muscle cells in vascular diseases. Am J Physiol Heart Circ Physiol. 2020;319(3):H613-h631.
36. Emini Veseli B, Perrotta P, De Meyer GRA, Roth L, Van der Donckt C, Martinet W, De Meyer GRY. Animal models of atherosclerosis. Eur J Pharmacol. 2017;816:3–13.
37. Daugherty A, Manning MW, Cassis LA. Angiotensin II promotes atherosclerotic lesions and aneurysms in apolipoprotein E-deficient mice. J Clin Invest. 2000;105(11):1605–12.
38. Weiss D, Kools JJ, Taylor WR. Angiotensin II-induced hypertension accelerates the development of atherosclerosis in apoE-deficient mice. Circulation. 2001;103(3):448–54.
39. Gopal K, Kumar K, Nandini R, Jahan P, Kumar MJM. High fat diet containing cholesterol induce aortic aneurysm through recruitment and proliferation of circulating agranulocytes in apoE knock out mice model. J Thromb Thrombolysis. 2010;30(2):154–63.
40. Li JJ, Chen JL. Inflammation may be a bridge connecting hypertension and atherosclerosis. Med Hypotheses. 2005;64(5):925–9.
41. Luo F, Zhou XL, Li JJ, Hui RT. Inflammatory response is associated with aortic dissection. Ageing Res Rev. 2009;8(1):31–5.
42. Sbarouni E, Georgiadou P, Analitis A, Voudris V. High neutrophil to lymphocyte ratio in type A acute aortic dissection facilitates diagnosis and predicts worse outcome. Expert Rev Mol Diagn. 2015;15(7):965–70.

43. Kalkan ME, Kalkan AK, Gündeş A, Yanartaş M, Oztürk S, Gurbuz AS, Ozturk D, Iyigun T, Akcakoyun M, Emiroglu MY, et al. Neutrophil to lymphocyte ratio: a novel marker for predicting hospital mortality of patients with acute type A aortic dissection. Perfusion. 2017;32(4):321–7.
44. Zhang H, Guo J, Zhang Q, Yuan N, Chen Q, Guo Z, Hou M. The potential value of the neutrophil to lymphocyte ratio for early differential diagnosis and prognosis assessment in patients with aortic dissection. Clin Biochem. 2021;97:41–7.
45. Rombouts KB, van Merrienboer TAR, Ket JCF, Bogunovic N, van der Velden J, Yeung KK. The role of vascular smooth muscle cells in the development of aortic aneurysms and dissections. Eur J Clin Invest. 2022;52(4): e13697.
46. Silvestre-Roig C, Braster Q, Wichapong K, Lee EY, Teulon JM, Berrebeh N, Winter J, Adrover JM, Santos GS, Froese A, et al. Externalized histone H4 orchestrates chronic inflammation by inducing lytic cell death. Nature. 2019;569(7755):236–40.